Solid-State Electronics 199 (2023) 108493

Contents lists available at ScienceDirect

Solid State Electronics

journal homepage: www.elsevier.com/locate/sse

Insights into few-atom conductive bridging random access memory cells with a combined force-field/*ab initio* scheme☆

J. Aeschlimann *, M.H. Bani-Hashemian, F. Ducry, A. Emboras, M. Luisier

Integrated Systems Laboratory, ETH Zürich, Gloriastrasse 35, 8092 Zürich, Switzerland

ARTICLE INFO

Keywords:
CBRAM
Resistive switching
Amorphous SiO_2
Force-field molecular dynamics
Ab initio quantum transport

ABSTRACT

We present a simulation framework to simulate the switching behavior of Ag/a-SiO_2 conductive bridging random access memories (CBRAM). Whereas the dynamics of the switching process is investigated with classical molecular dynamics simulations using a force-field, the electrical properties are determined through *ab initio* calculations. With a structural analysis of the oxide, we shed light on the switching mechanism, which relies on preferred channels containing wide SiO_2 rings through which Ag^+ ions migrate. Also, we demonstrate that moving only few atoms in such channels can change the resistance state by several orders of magnitude.

1. Introduction

Resistive random access memories (ReRAM) such as conductive bridging RAM (CBRAM) have attracted a lot of attention due to their non-volatility and fast switching speeds, providing a promising alternative to today's leading memory technologies such as flash. CBRAM cells are composed of a metal/oxide/metal structure where the typically amorphous insulating layer can be switched between a high- and low-resistance state through the reversible growth of a metallic filament upon application of an external potential (Fig. 1). To drive this technology towards its limits, the device sizes have been scaled down such that only few atoms are involved in their ON/OFF switching processes [1]. To increase the device performance and reliability, a clear understanding of the switching mechanism is needed at the atomic level. Models based on molecular dynamics have been suggested to investigate the migration of metal ions through the oxide [2]. Such approaches typically include a subsequent percolation analysis of the filament atoms to identify the ON- and OFF-states without considering the actual geometry and electronic structure of the filament.

In this work, we present a model for Ag/a-SiO_2 cells taking advantage of force-field molecular dynamics (FFMD). In contrast to *ab initio* MD (AIMD) [3], it is possible to simulate time lengths of several nanoseconds with FFMD, covering full SET and RESET processes. To determine the resistance state of the obtained filamentary structures, we then perform *ab initio* quantum transport (QT) calculations. Through this scheme, we benefit from both the computational efficiency of FF-based methods and the accuracy of *ab initio* calculations. With a structural analysis of the amorphous oxide, we identify preferred migration paths for Ag^+ ions during the switching process. We further demonstrate that the device can switch its resistance state by moving only few atoms.

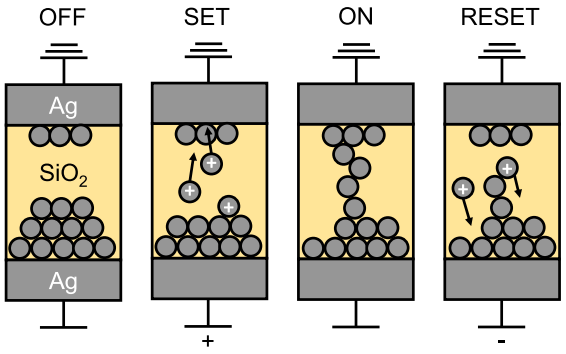

Fig. 1. Illustration of the switching process occurring in CBRAM cells. Typically, the cell is made of an inert, e.g., Pt, and of an active, e.g., Ag electrode. Here, for simplicity, it is built of two Ag electrodes and an insulating a-SiO_2 layer in between through which an Ag filament grows and dissolves, depending on the applied voltage.

2. Approach

Ag/a-SiO_2/Ag cells have been created by placing two Ag electrodes with a cross section of 2.06×2.04 nm^2 around a layer of amorphous

☆ The review of this paper was arranged by Francisco Gamiz.

* Corresponding author.
E-mail address: aejan@iis.ee.ethz.ch (J. Aeschlimann).

https://doi.org/10.1016/j.sse.2022.108493

Available online 28 October 2022

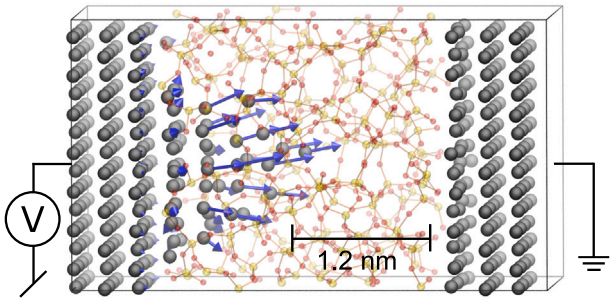

Fig. 2. Schematic view of the investigated Ag/a-SiO_2/Ag CBRAM cell. The Ag, Si, and O atoms are displayed as gray, yellow, and red spheres, respectively. A truncated cone-shaped Ag filament is inserted into the oxide as a seed, leaving a gap of 1.2 nm between the filament tip and the counter electrode. The blue arrows represent the local electric field to which the Ag filament atoms are exposed when an external potential of $V = +7$ V is applied to the left electrode while the right one remains grounded. (For interpretation of the references to colour in this figure legend, the reader is referred to the web version of this article.)

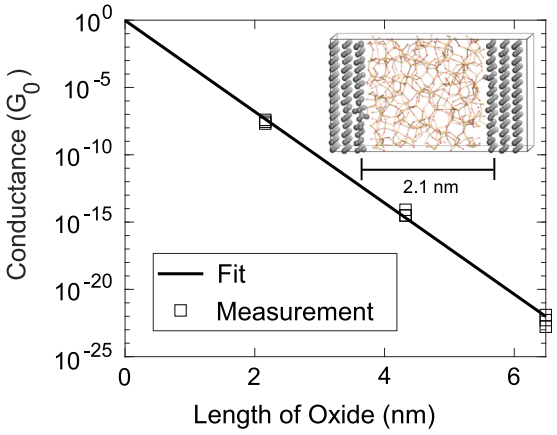

Fig. 3. Electrical conductance (in conductance quantum G_0) of pristine Ag/a-SiO_2/Ag CBRAM structures as a function of the length of the oxide. Three different samples similar to the one shown in the inset were constructed with three different oxide lengths each. The average conductance decreases exponentially with the length of the oxide.

SiO_2 (a-SiO_2) with a density of 2.20 g/cm^3. This symmetrical CBRAM stack was chosen for computational convenience to reduce the complexity of the FF. Additionally, two different electrode materials, as typically used in experiments, could cause unphysical strain-induced defect states in the SiO_2 band gap through lattice mismatch and alter the conductivity of the oxide. The a-SiO_2 is generated by the melt-and-quench method [4]. Only samples free from structural defects were selected to avoid negative effects such as Fermi level pinning in the QT calculations. A truncated cone-shaped filament made of 36 to 50 Ag atoms was then inserted into the oxide as a seed, leaving a gap of 1.2 nm between the electrodes (see Fig. 2). One-fold coordinated oxide atoms at the interface to the filament were removed to construct a smoother and more realistic interface.

All FFMD simulations were performed with QuantumATK S-2021.06 [5,6] and the moment tensor potential (MTP) framework [7] with a time step of 1 fs at 300 K. The MTP parameter file was trained using a set of representative AIMD trajectories of different Ag/SiO_2 interfaces, clusters, and filaments. The influence of the external electric potential is included by modifying the forces acting on each atom with an additional term $\vec{F}_{\text{ext}}(r_i) = q(r_i)\vec{E}$, where $q(r_i)$ and $\vec{E}$ are the atomic charge of atom i at position r_i and the applied electric field, respectively. The electric field is evaluated by a generalized Poisson solver [8] treating the various filament shapes accurately (Fig. 2). The charges on the Ag atoms are assigned based on their coordination number and whether they are connected to an electrode or dissolved in a-SiO_2. To find a relationship between coordination number and charge, 20 different CBRAM structures with the aforementioned embedded truncated cone were prepared. Then, the Mulliken charge and its coordination number to nearby Ag atoms were calculated for all Ag atoms using CP2K [9] and taken as a reference. Similarly, for dissolved metal ions, the Mulliken charge for single Ag^+ ions and small Ag clusters dissolved in cubes of a-SiO_2 with 1.5 nm length was evaluated. Unlike before, a charge equivalent to the number of Ag atoms was applied to mimic the ionic nature of the dissolved species.

For selected structures obtained by FFMD, *ab initio* QT calculations were performed to extract their resistance state. To do so, the structures were annealed for 0.1 ps with AIMD at 300 K. As a next step, the Hamiltonian and overlap matrices were prepared in CP2K using contracted Gaussian-type DZVP orbitals as basis set, the PBE exchange correlation functional [10], and GTH pseudopotentials [11]. They were finally passed to OMEN [12], a quantum transport device simulator that relies on density functional theory and the non-equilibrium Green's function (NEGF) formalism.

3. Results

To verify that the high-resistance state is not limited by intrinsic defects in the oxide, we first performed QT calculations of pristine oxide structures with three different lengths. To eliminate the influence of the metal/oxide interfaces, equivalent a-SiO_2 blocks of 2.1 nm length were repeated one, two, and three times. Fig. 3 shows that the conductance decreases exponentially with longer oxides, indicating that the current is dominated by tunneling effects and not by structural defect states.

FFMD simulations under an applied voltage of +7 V show the growth of a filament consisting of a single atom chain towards the counter electrode (Fig. 4(a)). The growth occurs incrementally with bursts lasting only a few picoseconds in which the atoms move individually or as a chain towards the counter electrode by several angstrom. During the remaining time the shape and length of the filament does not change. Fig. 4(b) demonstrates that different resistance levels can be achieved during the SET process, depending on the geometry of the filament and its distance to the counter electrode. The movement of one single atom can lead to a change in resistance of more than one order of magnitude. Unstable configurations may be reached that results in partial disruption of the filament and a temporary decrease in conductance.

After 6.5 ns, the device reached its ON-state with a bridging filament containing as few as five atoms originally located at the tip of the truncated cone. An ON/OFF conductance ratio of 10^4 is recorded. Fig. 5 confirms the conductive nature of the filament. When a read current of 0.1 V is applied, the current density is maximum in the single atom chain. The ON-state was kept during 2 ns without any applied voltage before the filament was disrupted by applying −1 V, which pushes the bridging atoms back. Similar to the SET process, the resistance does not change gradually during the RESET process. In fact, bursts of disruption are noted, leading to a change in resistance of several orders of magnitude within only a few picoseconds. The negative RESET voltage confirms a non-volatile switching behavior. A reason for the high SET voltage (+7 V) compared to the low RESET voltage (−1 V) could rely on the simplified modeling of the redox reaction taking place at the Ag/a-SiO_2 interface, which is solely driven by $\vec{F}_{\text{ext}}$. The assignment of the atomic charges based on the coordination number potentially underestimates the actual charges being present during the redox reactions at the Ag/a-SiO_2 interfaces. Consequently, the SET voltage might be overestimated.

Unlike its crystalline counterparts such as α-quartz, a-SiO_2 possesses a broad Si–O bond length and Si–O–Si angle distribution. This has a direct impact on the atomic structure, which in its core can be regarded

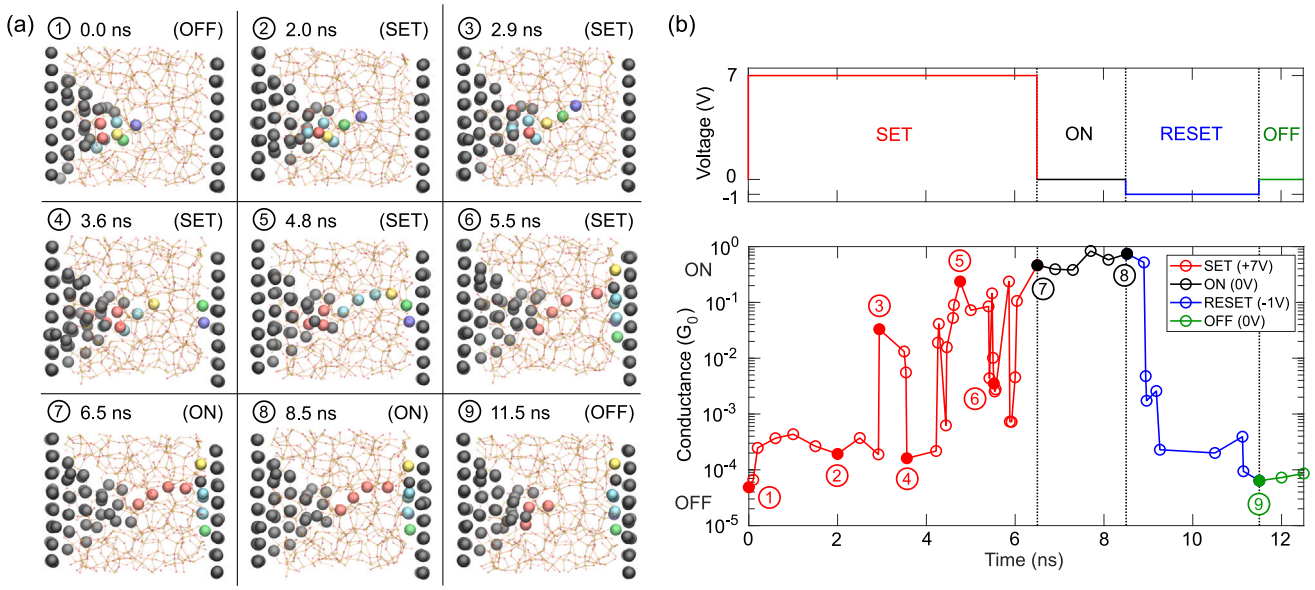

Fig. 4. (a) Evolution of the bridging filament in an Ag/a-SiO_2 CBRAM cell as a function of time. The structure displayed in Fig. 2 is used as starting point. Ag atoms are displayed as gray spheres, those contributing to the filament are colored. The a-SiO_2 matrix is shown in orange. To simulate the SET process, FFMD was performed at 300 K for 6.5 ns under an applied voltage of +7 V that is applied to the left electrode while the right one is grounded. A filament consisting of atoms originally located at the tip of the truncated cone grows into the oxide as a chain of single atoms. When the applied voltage is set to −1 V, the filament ruptures and the Ag atoms forming the filament move backwards. (b) Time evolution of the applied voltage and corresponding CBRAM conductance state. Following an unstable phase, the filament finally reaches the ON-state after 6.5 ns. This state is kept during 2 ns. The RESET to the OFF-state is achieved in less than 0.5 ns. The ON/OFF conductance ratio of the device is equal to 10^4. (For interpretation of the references to colour in this figure legend, the reader is referred to the web version of this article.)

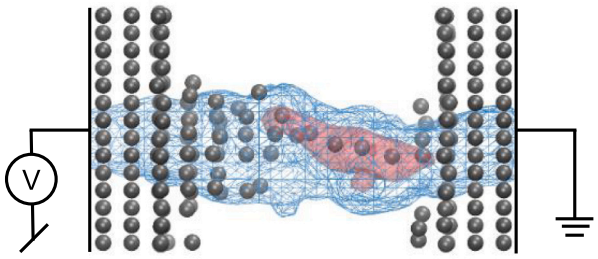

Fig. 5. Ballistic current (illustrated as two different isosurfaces) through the structure representing the ON-state displayed in Fig. 4(a). An external read voltage of $V = 0.1$ V was applied. The maximum current is measured in the single atom chain of the filament.

as connected silica rings. A ring analysis on the basis of the King criteria [13] for the modeled a-SiO_2 structures reveals that silica rings containing three to nine Si atoms are present, with six-fold rings being the most common ones (Fig. 6(a)). Additionally, a-SiO_2 exhibits pores of different sizes in which the Ag^+ ions can reside. This stochastic inhomogeneity of the structure is the key for the switching process in Ag/a-SiO_2 CBRAM cells.

By comparing the ring sizes with the migration trajectories of Ag^+ ions during the switching process, a correlation between the filament growth path and the local silica ring distribution can be noted. Similarly to the observation from diffusion studies [14], Ag^+ ions require more energy to pass through tighter rings than looser ones. Hence, the filament particularly forms in regions of many silica rings containing at least six Si atoms, whereas migration through five-fold rings could not be observed. Fig. 6(b)–(c) illustrate these findings exemplarily for a structure that did not result in a bridging filament. A filament started to grow through six- and eight-fold silica rings, filling up pores. However, denser areas with tighter rings close to the interface to the right contact prevented the filament from growing further.

Therefore, the filament probability of becoming a bridge between both electrodes directly depends on the local structure of the oxide. The silver ions can only find a continuing channel if the SiO_2 regions to pass are locally sparse enough. Between passages through two wide SiO_2 rings, the Ag^+ ions reside in pores and are stabilized through cohesion by adjacent Ag filament atoms.

4. Conclusions

We have developed a model to simulate the growth and dissolution process of bridging filaments in Ag/a-SiO_2 CBRAM cells using FFMD. Based on a SiO_2 ring analysis, we have identified specific paths through which Ag^+ ions preferably migrate. The resistance states of these devices have been evaluated through *ab initio* QT methods, highlighting out that the movement of only few atoms can lead to resistance changes of several orders of magnitude.

Declaration of competing interest

The authors declare that they have no known competing financial interests or personal relationships that could have appeared to influence the work reported in this paper.

Data availability

Data will be made available on request.

Acknowledgment

We thank Julian Schneider (Synopsys Inc.) for his help in the parameterization of the force-field. This research was supported by the Werner Siemens Stiftung, Switzerland and by the Swiss National Supercomputing Centre (CSCS) under Projects s714 and s1119.

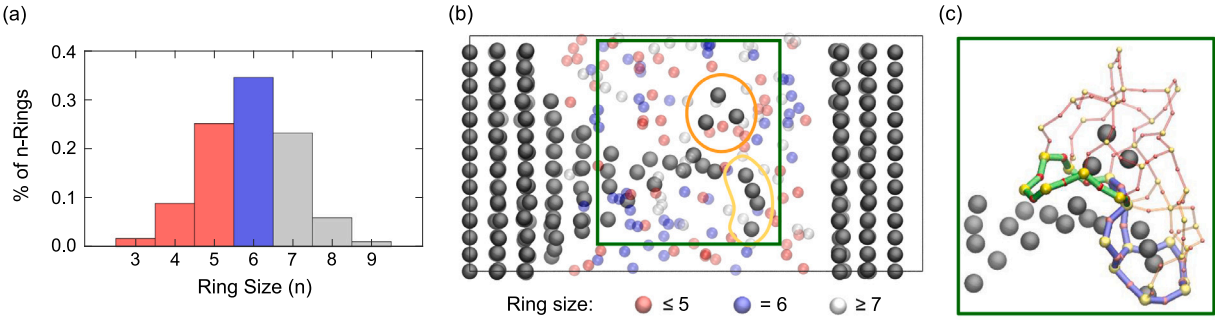

Fig. 6. (a) Ring size distribution of the a-SiO_2 structure that was used to create the CBRAM cell displayed in Fig. 2. A *n*-ring is defined as a ring containing *n* Si and O atoms each. (b) Illustration of the filament growth in an Ag/a-SiO_2 CBRAM structure that did not result in a bridging filament. The oxide consists of inhomogeneously distributed SiO_2 rings whose centers are colored according to their ring size. The Ag filament (gray spheres) preferentially grows through regions with a sparser ring population, while it is prevented from entering dense regions with tight (five-fold) rings at the interface to the right contact. (c) Zoom into the green rectangle in (b). It can be seen that the upper part (orange circle in (b)) of the filament has entered a pore (depicted by the red network) through an eight-fold SiO_2 ring (green). The bottom part (yellow circle in (b)) has grown through two six-fold SiO_2 rings (blue) whereas tighter rings could not be passed. (For interpretation of the references to colour in this figure legend, the reader is referred to the web version of this article.)

References

[1] Cheng B, Emboras A, Salamin Y, Ducry F, Ma P, Fedoryshyn Y, Andermatt S, Luisier M, Leuthold J. Ultra compact electrochemical metallization cells offering reproducible atomic scale memristive switching. Commun Phys 2019;2(1):28.

[2] Onofrio N, Guzman D, Strachan A. Atomic origin of ultrafast resistance switching in nanoscale electrometallization cells. Nat Mater 2015;14(4):440–6.

[3] Akola J, Konstantinou K, Jones RO. Density functional simulations of a conductive bridging random access memory cell: Ag filament formation in amorphous GeS_2. Phys Rev Mater 2022;6:035001.

[4] Ducry F, Aeschlimann J, Luisier M. Electro-thermal transport in disordered nanostructures: a modeling perspective. Nanoscale Adv 2020;2:2648–67.

[5] Smidstrup S, Markussen T, Vancraeyveld P, Wellendorff J, Schneider J, Gunst T, Verstichel B, Stradi D, Khomyakov PA, Vej-Hansen UG, Lee M-E, Chill ST, Rasmussen F, Penazzi G, Corsetti F, Ojanperä A, Jensen K, Palsgaard MLN, Martinez U, Blom A, Brandbyge M, Stokbro K. QuantumATK: An integrated platform of electronic and atomic-scale modelling tools. J Phys: Condens Matter 2020;32:015901.

[6] Schneider J, Hamaekers J, Chill ST, ren Smidstrup S, Bulin J, Thesen R, Blom A, Stokbro K. ATK-ForceField: a new generation molecular dynamics software package. Modelling Simulation Mater Sci Eng 2017;25(8):085007.

[7] Shapeev AV. Moment tensor potentials: A class of systematically improvable interatomic potentials. Multiscale Model Simul 2016;14(3):1153–73.

[8] Bani-Hashemian MH, Brück S, Luisier M, VandeVondele J. A generalized Poisson solver for first-principles device simulations. J Chem Phys 2016;144(4):044113.

[9] Kühne TD, Iannuzzi M, Del Ben M, Rybkin VV, Seewald P, Stein F, Laino T, Khaliullin RZ, Schütt O, Schiffmann F, Golze D, Wilhelm J, Chulkov S, Bani-Hashemian MH, Weber V, Borštnik U, Taillefumier M, Jakobovits AS, Lazzaro A, Pabst H, Müller T, Schade R, Guidon M, Andermatt S, Holmberg N, Schenter GK, Hehn A, Bussy A, Belleflamme F, Tabacchi G, Glöß A, Lass M, Bethune I, Mundy CJ, Plessl C, Watkins M, VandeVondele J, Krack M, Hutter J. CP2K: An electronic structure and molecular dynamics software package - Quickstep: Efficient and accurate electronic structure calculations. J Chem Phys 2020;152(19):194103.

[10] Perdew JP, Burke K, Ernzerhof M. Generalized gradient approximation made simple. Phys Rev Lett 1996;77:3865–8.

[11] Goedecker S, Teter M, Hutter J. Separable dual-space Gaussian pseudopotentials. Phys Rev B 1996;54:1703–10.

[12] Luisier M, Schenk A, Fichtner W, Klimeck G. Atomistic simulation of nanowires in the $sp^3d^5s^*$ tight-binding formalism: From boundary conditions to strain calculations. Phys Rev B 2006;74:205323.

[13] King SV. Ring configurations in a random network model of vitreous silica. Nature 1967;213(5081):1112–3.

[14] Patel K, Cottom J, Bosman M, Kenyon A, Shluger A. An oxygen vacancy mediated Ag reduction and nucleation mechanism in SiO_2 RRAM devices. Microelectron Reliab 2019;98:144–52.